International Journal of Mass Spectrometry 378 (2015) 76–85

Contents lists available at ScienceDirect

International Journal of Mass Spectrometry

journal homepage: www.elsevier.com/locate/ijms

# Infrared multiple photon dissociation action spectroscopy of sodium cationized halouracils: Effects of sodium cationization and halogenation on gas-phase conformation

C.M. Kaczan [a], A.I. Rathur [a], R.R. Wu [a], Y. Chen [a], C.A. Austin [a], G. Berden [b], J. Oomens [b,c], M.T. Rodgers [a,*]

[a] Department of Chemistry, Wayne State University, Detroit, MI 48202, USA
[b] Radboud University Nijmegen, Institute for Molecules and Materials, FELIX Facility, Toernooiveld 7, 6525 ED Nijmegen, The Netherlands
[c] van't Hoff Institute for Molecular Sciences, University of Amsterdam, Amsterdam, The Netherlands

ARTICLE INFO

*Article history:*
Received 6 May 2014
Received in revised form 4 July 2014
Accepted 4 July 2014
Available online 9 July 2014

**In honor of Veronica M. Bierbaum on the occasion of her 65th birthday, in thanks for her numerous contributions to gas-phase ion thermochemistry, and in appreciation for her friendship, mentoring and support throughout my professional career.**

*Keywords:*
Density function theory
Fourier transform ion cyclotron resonance mass spectrometry
Halouracils
Infrared multiple photon dissociation
Sodium cation

ABSTRACT

The gas-phase structures of sodium cationized complexes of 5- and 6-halo-substituted uracils are examined via infrared multiple photon dissociation (IRMPD) action spectroscopy and theoretical electronic structure calculations. The halouracils examined in this investigation include: 5-flourouracil, 5-chlorouracil, 5-bromouracil, 5-iodouracil, and 6-chlorouracil. Experimental IRMPD action spectra of the sodium cationized halouracil complexes are measured using a 4.7 T Fourier transform ion cyclotron resonance mass spectrometer coupled to the FELIX free electron laser (FEL). Irradiation of the mass selected sodium cationized halouracil complexes by the FEL was carried out over the range of frequencies extending from 950 to 1900 $cm^{-1}$. Theoretical linear IR spectra predicted for the stable low-energy conformations of the sodium cationized halouracils, calculated at B3LYP/6-31G(d) level of theory, are compared with the measured IRMPD action spectra to identify the structures accessed in the experiments. Relative stabilities of the low-energy conformations are determined from single-point energy calculations performed at the B3LYP/6-311+G(2d,2p) level of theory. The evolution of IRMPD spectral features as a function of the size (F, Cl, Br, and I) and position (5 versus 6) of the halogen substituent are examined to elucidate the effects of the halogen substituent and noncovalent interactions with sodium cations on the structure of the nucleobase. Present results are compared with results from energy-resolved collision-induced dissociation and IRMPD action spectroscopy studies previously reported for the protonated and sodium cationized forms of uracil, and halo-, methyl-, and thioketo-substituted uracils. The present results suggest that only a single conformer is accessed for all of the 5-halouracil complexes, whereas multiple conformers are accessed for the $Na^+$(6ClU) complex. In all cases, the experimental IRMPD action spectra confirm that the sodium cation binds to the O4 carbonyl oxygen atom of the canonical diketo tautomer in the ground-state conformers, and gains additional stabilization via chelation interactions with the halogen substituent in the complexes to the 5-halouracils as predicted by theory.

© 2014 Elsevier B.V. All rights reserved.

## 1. Introduction

The 5- and 6-halouracils have been shown to exhibit antitumor and antiviral activities [1–18]. The ability of 5- and 6-halouracils to control damage to healthy tissues during radiation therapy has been evaluated [1]. 5-Chlorouracil and 5-bromouracil have been studied for their use in the treatment of inflammatory tissue [2]. 5-Fluorouracil is currently employed in colorectal, breast, and head and neck cancer treatments [3–5] due to its ability to inhibit thymine synthase, and thus prevent the conversion of uracil to thymine [4,5]. 5-Fluorouracil is incorporated into DNA by DNA polymerase and excised by DNA glycosylase leading to toxic abasic sites and subsequent DNA strand breaks [5]. Fluorine is similar in size to a hydrogen atom, and like uracil 5-fluorouracil is excised by DNA glycosylase, whereas chlorine and bromine are similar in size to a methyl group such that 5-chlorouracil and 5-bromouracil, like thymine, are not excised by DNA glycosylase. Similar mechanisms for 5-chlorouracil and 5-bromouracil utilizing thymine DNA glycosylase have been suggested [19]. However, the mechanisms of antitumor and antiviral actions of these nucleobases are not well understood. Thus, research into the structures and binding interactions of halouracils are of great importance in pharmaceutical research.

* Corresponding author. Tel.: +1 3135772431; fax: +1 3135778822.
*E-mail address:* mrodgers@chem.wayne.edu (M.T. Rodgers).

http://dx.doi.org/10.1016/j.ijms.2014.07.016
1387-3806/© 2014 Elsevier B.V. All rights reserved.

Sodium cations are essential to biological systems as they play vital roles in heart activity, blood and fluid regulation, nerve impulse transmission, and metabolic functions. One of the most recognized functions of sodium cations is their role in creating ion gradients with potassium ions. Secondary active transport utilizes a $Na^+/K^+$ ion gradient to transport amino acids, nucleotides, and other biological molecules across cell membranes. Voltage-gated ion channels found in neurons also utilize a $Na^+/K^+$ ion gradient to pass electrical signals from neuron to neuron [20]. Sodium cations are also involved in nucleic acid chemistry exhibiting charge neutralization and noncovalent interactions that lead to the stabilization of DNA and RNA [21,22]. The presence of metal cations influences the function, stability, and conformational behavior of surrounding molecules. Metal cations binding to the nucleobase can produce more significant effects on DNA and RNA conformation than those binding to the phosphate backbone [23]. The formation and stabilization of minor nucleobase tautomers can be caused by the presence of metal cations [24]. These nucleobase modifications can potentially lead to base mispairing and cause errors in the transfer of genetic information [25].

The properties and characteristics of protonated and sodium cationized uracil and modified uracils have been extensively studied [25–31]. Previous infrared multiple photon dissociation (IRMPD) action spectroscopy studies by Crampton et al. of protonated halouracils [26], Salpin et al. of uracil [27], and Nei et al. of uracil, thioketo-, and methylthioketo-uracils [28] found that protonation preferentially stabilizes minor noncanonical tautomers of all of the nucleobases examined thus far except 4-thiouracil. In contrast, previous CID and theoretical studies by Rodgers and Armentrout of sodium cationized uracil [29] and by Yang et al. of sodium cationized methyl- [25], thioketo- [30], and halo-substituted uracils, [31] suggest that the ground-state structures involve the canonical tautomers and the dominant CID processes observed arise from loss of the intact neutral nucleobase. Similarly, the IRMPD study by Nei et al. of sodium cationized uracil, thioketo- and methylthioketo-uracils found the ground-state structures to involve the canonical tautomer of the nucleobase except in complexes of 4-thiouracil and 2,4-dithiouracil, where minor tautomers are preferentially stabilized [32].

Structural information regarding the sodium cationized halouracils in the previous CID study was inferred by comparison of measured and theoretically estimated bond dissociation energies [31]. In the current study, IRMPD action spectroscopy techniques are used to probe the structures of sodium cationized halouracils. The influences of halogenation and noncovalent interactions with sodium cations on the gas-phase tautomeric conformations of the halouracils are also examined. The structures and relative stabilities at 298 K of all possible tautomers of the sodium cationized halouracils are calculated. The halouracils investigated in this study include: 5-fluorouracil (5FU), 5-chlorouracil (5ClU), 5-bromouracil (5BrU), 5-iodouracil (5IU), and 6-chlorouracil (6ClU), allowing the influence of the size and position of the halogen substituent on the structure of sodium cationized halouracils to be elucidated. The canonical structures of neutral uracil and the halouracils investigated here are shown in Fig. 1. In order to definitively determine the ground-state and low-energy tautomeric conformations of the sodium cationized forms of these nucleobases, IRMPD action spectra of these complexes are measured and compared to theoretical linear IR spectra of the stable low-energy structures of the sodium cationized halouracil complexes derived from electronic structure calculations performed at the B3LYP/6-31G(d) level of theory.

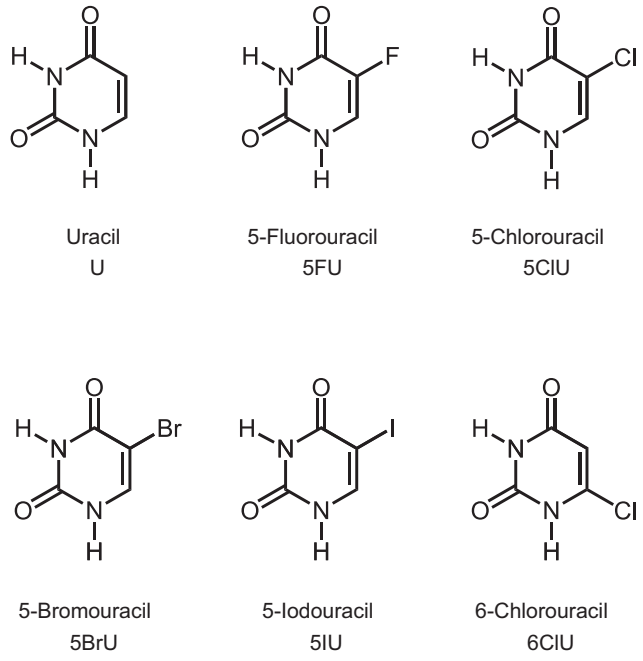


**Fig. 1.** Structures of uracil (U) and the halouracils (*x*U), where *x*U = 5FU, 5ClU, 5BrU, 5IU and 6ClU.

## 2. Experimental and computational

### 2.1. Mass spectrometry and photodissociation

Experimental studies were carried out at the FELIX facility using a 4.7 T Fourier transform ion cyclotron resonance mass spectrometer (FT-ICR MS) coupled to a free electron laser (FEL) [33–35]. IRMPD action spectra were obtained for five $Na^+$(*x*U) complexes, where *x*U represents 5FU, 5ClU, 5BrU, 5IU, and 6ClU. 5FU and 5BrU were obtained from Sigma–Aldrich, whereas 5ClU, 5IU, and 6ClU were obtained from TCL Tokyo Kasei. Solution conditions employed for the samples examined were 1–2 mM nucleobase with 1–2 mM NaCl in 50%:50% to 80%:20% MeOH:$H_2O$ solutions.

Sample solutions were delivered via a syringe pump to a Micromass z-spray electrospray ionization (ESI) source at a flow rate of 10 μL/min and a needle voltage of 3.2–3.4 kV. Ions emanating from the ESI source were accumulated in a hexapole ion trap for several seconds, and then pulse extracted and sent through a quadrupole bender into an octopole ion guide. Ions were slowed within the octopole ion guide by traveling up a potential difference created by a negative dc bias with relative ground potential at the ICR cell to allow for easy capture by gated ion trapping [33]. Once ions were trapped within the ICR cell, stored waveform inverse Fourier transform (SWIFT) excitation was used to isolate the desired sodium cationized halouracil complex from unwanted ions formed in the ionization process. As chlorine and bromine exist naturally in two isotopes, complexes with both isotopes were isolated and used to produce greater precursor ion intensity and to properly identify the desired precursor ion. Selected ions were irradiated by the FEL (entering from the back of the ICR cell) at pulse energies of ~40 mJ per macropulse of 5 μs duration for 3 s, corresponding to interaction with 15 macropulses over the wavelength range extending from 10.5 μm (950 $cm^{-1}$) to 5.3 μm (1900 $cm^{-1}$) to induce photodissociation. Dissociation occurs when the wavelength of the radiation corresponds to a resonant absorption mode of the precursor ion. Precursor ions absorb photons and distribute the absorbed energy throughout the

internal modes of the ion by intramolecular vibrational redistribution until the dissociation threshold is reached. The absorption of tens to hundreds of photons is generally required for dissociation. The multiple pass arrangement allows for increased interaction with the FEL. The intensities of the precursor and photofragment ions were monitored as a function of the FEL wavelength. The IRMPD yield is calculated from the precursor ion intensity ($I_p$) along with the sum of the fragment ion intensities ($I_{f_i}$) at each frequency as shown in Eq. (1).

$$\text{IRMPD yield} = \frac{(\sum_i I_{f_i})}{(I_p + \sum_i I_{f_i})} \quad (1)$$

The IRMPD yield was power corrected using linear normalization to account for changes in the power of the laser as a function of photon energy, (i.e., the wavelength of the FEL). This total fragment yield was then plotted as a function of the wavelength, producing the IRMPD spectrum.

### 2.2. Computational details

Theoretical calculations were performed using the Gaussian 03 suite of programs [36] to determine all stable tautomeric conformations of the neutral and sodium cationized uracil and halouracils. Structures and relative stabilities of the 13 stable tautomeric conformations of each of the neutral halouracils can be found in Fig. S1 along with the 13 tautomers of uracil (U) previously reported [28]. The structures and relative stabilities of a total of 187 stable tautomeric conformations of the sodium cationized halouracils including: 35 of $Na^+$(5FU), 36 $Na^+$(5ClU), 34 $Na^+$(5BrU), 31 $Na^+$(5IU), 27 $Na^+$(6ClU), and the 24 tautomers of sodium cationized uracil that were previously reported [28] can be found in Fig. S2. Optimized structures and harmonic vibrational frequencies were calculated at the B3LYP/6-31G(d) level of theory. Single point energies used to determine the relative enthalpies at 0 K for each conformer were calculated at the B3LYP/6-311+G(2d,2p) level of theory. Thermal corrections to convert 0 K enthalpies to enthalpies and Gibbs free energies at 298 K were determined using standard formulae (based on rigid rotor and harmonic oscillator approximations) and the rotational constants and vibrations frequencies determined at the B3LYP/6-31G(d) level of theory. In the case of 5-iodouracil an iodine effective core potential was used to decrease the computational effort by focusing on only valence electrons of the iodine atom, whereas the core electrons are represented by the LANL2DZ and modified LANL2DZ effective core potentials [37,38]. Theoretical linear IR spectra were generated using the harmonic vibrational frequencies and IR intensities. The vibrational frequencies are scaled by a factor of 0.96 as recommended by Foresman and Frisch [39]. Calculated vibrational frequencies are convoluted with a 20 $cm^{-1}$ fwhm Gaussian line shape for comparison to the measured IRMPD spectra.

## 3. Results

### 3.1. IRMPD action spectroscopy

In all cases, IRMPD of the $Na^+$(*x*U) complexes leads to loss of the intact nucleobase and detection of $Na^+$ at $m/z = 23$. IRMPD action spectra of the $Na^+$(*x*U) complexes measured in this work along with the spectrum for the $Na^+$(U) complex previously reported [32] are compared in Fig. 2. As can be seen in the figure, these complexes exhibit highly parallel spectral features. However, the spectra exhibit systematic shifting of the band positions of several features allowing facile differentiation of these complexes. The intense band at ~1801 $cm^{-1}$ in the IRMPD spectrum of $Na^+$(U) is slightly blue

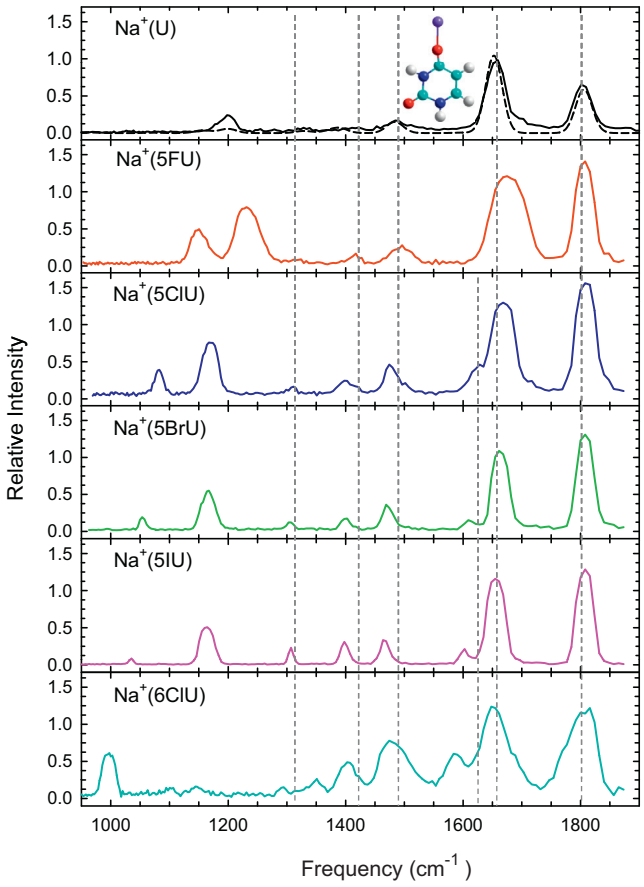


**Fig. 2.** IRMPD action spectra of $Na^+$(U) and $Na^+$(*x*U) complexes, where *x*U = 5FU, 5ClU, 5BrU, 5IU, and 6ClU. The structure and theoretical linear IR spectrum calculated at the B3LYP/6-31G(d) level of theory and convoluted with a 20 $cm^{-1}$ fwhm Gaussian line shape (dotted line) are shown for the most stable conformer of $Na^+$(U). Data for $Na^+$(U) is taken from reference [28].

shifted to ~1808 $cm^{-1}$ for all of the $Na^+$(*x*U) complexes. The intense band observed at ~1659 $cm^{-1}$ for $Na^+$(U), is blue shifted by 16 $cm^{-1}$ for $Na^+$(5FU) to ~1675 $cm^{-1}$. Relative to $Na^+$(5FU), this band is increasingly red shifted for the other $Na^+$(5XU) complexes as the size of the halogen substituent increases, and appears at the lowest frequency for the $Na^+$(6ClU) complex. The red shifting of this intense band as well as the appearance of a new feature in the IRMPD spectra of the $Na^+$(*x*U) complexes that also red shifts increasingly as the size of the halogen substituent increases, leads to narrowing of this broad feature and the appearance and eventual resolution of two bands in the IRMPD spectra of the $Na^+$(*x*U) complexes. In the IRMPD spectrum of $Na^+$(5FU), the new feature is masked by the intense band between ~1648 and 1675 $cm^{-1}$, whereas for $Na^+$(5ClU) a shoulder to the red is observed at ~1628 $cm^{-1}$. The corresponding band is further red shifted and observed as a separate band at ~1608 $cm^{-1}$ in the IRMPD spectrum of $Na^+$(5BrU), and is even further red shifted to 1602 $cm^{-1}$ for $Na^+$(5IU) and to 1584 $cm^{-1}$ for $Na^+$(6ClU). Three peaks of low intensity appear in the IRMPD spectra of $Na^+$(U) and the $Na^+$(5*x*U) complexes between ~1295 and 1496 $cm^{-1}$, with the band appearing at the lowest frequency being the weakest and that at the highest frequency the most intense. The weak band at ~1485 $cm^{-1}$ for $Na^+$(U) is blue shifted by 11 $cm^{-1}$ to 1496 $cm^{-1}$ for $Na^+$(FU). In contrast, this band is red shifted for the other halouracils, by 10 $cm^{-1}$ to 1474 $cm^{-1}$ for $Na^+$(5ClU) and $Na^+$(6ClU), 18 $cm^{-1}$ to 1468 $cm^{-1}$ for $Na^+$(5BrU), and 21 $cm^{-1}$ to 1464 $cm^{-1}$ for $Na^+$(IU). The band observed at 1417 $cm^{-1}$ in the IRMPD spectra of $Na^+$(U) and $Na^+$(5FU) is red shifted by 14 $cm^{-1}$ to 1403 $cm^{-1}$ for $Na^+$(5ClU), $Na^+$(5BrU), and $Na^+$(6ClU), and is further

red shifted by 19 $cm^{-1}$ to 1398 $cm^{-1}$ in the IRMPD spectrum of $Na^+$(5IU). The very weak band that appears at ~1328 $cm^{-1}$ in the IRMPD spectrum of $Na^+$(U), is red shifted by 17 $cm^{-1}$ for $Na^+$(5FU) and $Na^+$(5ClU) to 1311 $cm^{-1}$, by 21 $cm^{-1}$ for $Na^+$(5BrU) and $Na^+$(5IU) to 1307 $cm^{-1}$, and by 33 $cm^{-1}$ to 1295 $cm^{-1}$ for $Na^+$(6ClU). It cannot be determined from the spectra alone which of the two bands between 997 and 1231 $cm^{-1}$ for each of the halouracils corresponds to the band exhibited at 1198 $cm^{-1}$ for $Na^+$(U). Both features observed for the $Na^+$(5*x*U) complexes are increasingly red shifted such that the frequency difference between these two peaks also increases as the size of the halogen substituent increases. The higher energy feature exhibits a greater intensity for all of the 5-halouracils, whereas it is of lower intensity for $Na^+$(6ClU). $Na^+$(6ClU) exhibits new features at ~1350 and 1688 $cm^{-1}$ that are not observed in the spectra of the $Na^+$(5*x*U) complexes. It cannot be determined from the spectra alone which of the three bands at ~1000, 1110, and 1150 $cm^{-1}$ in the IRMPD spectrum of $Na^+$(6ClU) correspond to the two bands observed for each of the 5-halouracils. The IRMPD yield is greater for $Na^+$(6ClU) than $Na^+$(5ClU), which may suggest an increased density of states, reactivity, or the presence of multiple conformers in the experiments.

The position of the halogen substituent, 5 versus 6, in $Na^+$(5ClU) and $Na^+$(6ClU) can be readily differentiated by their IR spectra. Distinguishing features between the spectra include red shifting of the shoulder at 1628 $cm^{-1}$ observed for $Na^+$(5ClU) by 44 $cm^{-1}$ to 1584 $cm^{-1}$ for $Na^+$(6ClU). The two spectra can also be distinguished by the presence of two bands at ~1075 and 1175 $cm^{-1}$ for $Na^+$(5ClU), whereas $Na^+$(6ClU) exhibits a band at ~1000 $cm^{-1}$ of similar intensity and two low intensity features at ~1110 and 1150 $cm^{-1}$. $Na^+$(6ClU) also exhibits new features at ~1350 and 1688 $cm^{-1}$ that are not observed in the IRMPD spectrum of $Na^+$(5ClU), which further aid in the differentiation of these species.

### 3.2. Theoretical results

The 13 most stable tautomeric conformations of uracil and the halouracils are shown in Fig. 3, whereas those of the $Na^+$(U) and $Na^+$(*x*U) complexes are shown in Fig. 4. The B3LYP/6-31G(d) optimized structures and B3LYP/6-311+G(2d,2p) relative Gibbs free energies at 298 K of the stable low-energy tautomers of the 5-halouracils are included in Fig. S1 of the Supplementary Information, whereas those for the $Na^+$(U) and $Na^+$(*x*U) complexes are shown in Fig. S2. Relative enthalpies and Gibbs free energies calculated at the B3LYP/6-311+G(2d,2p) level of theory at 298 K including zero point energy and thermal corrections for the 12 most stable tautomers of the $Na^+$(*x*U) complexes along with those for the $Na^+$(U) complex previously reported [32] are listed in Table 1. In all cases, the ground-state tautomeric conformations of the sodium cationized halouracils are the $\mathbf{A^2}$ and $\mathbf{A^1}$ conformers shown in Fig. 4. These conformers result from binding of the sodium cation to the O4 carbonyl oxygen atom of the canonical **a** tautomers of the halouracils. In the case of the 5-halouracils, the sodium cation gains additional stabilization via chelation with the O4 carbonyl oxygen and the 5-halo-substituent, the $\mathbf{A^2}$ conformer, resulting in a ∠CONa$^+$ bond angle of 118.9–138.9° for the 5-halouracils. In contrast, the ∠CONa$^+$ bond angle is nearly linear (173.5°) in the $\mathbf{A^1}$ conformation of the $Na^+$(6ClU) complex.

#### 3.2.1. $Na^+$(5xU)

As discussed above, the ground-state structures of the $Na^+$(5*x*U) complexes are the $\mathbf{A^2}$ conformers shown in Fig. 4 resulting from sodium cationization of the **a** conformers of 5*x*U (Fig. S1). In these structures protons are bound to the N1, N3, and C6 atoms with the sodium cation chelating between the O4 carbonyl oxygen atom and 5-halo-substituent. Sodium cationization of the **a** conformers at the O2 position leads to the **D** conformers. These conformers lie

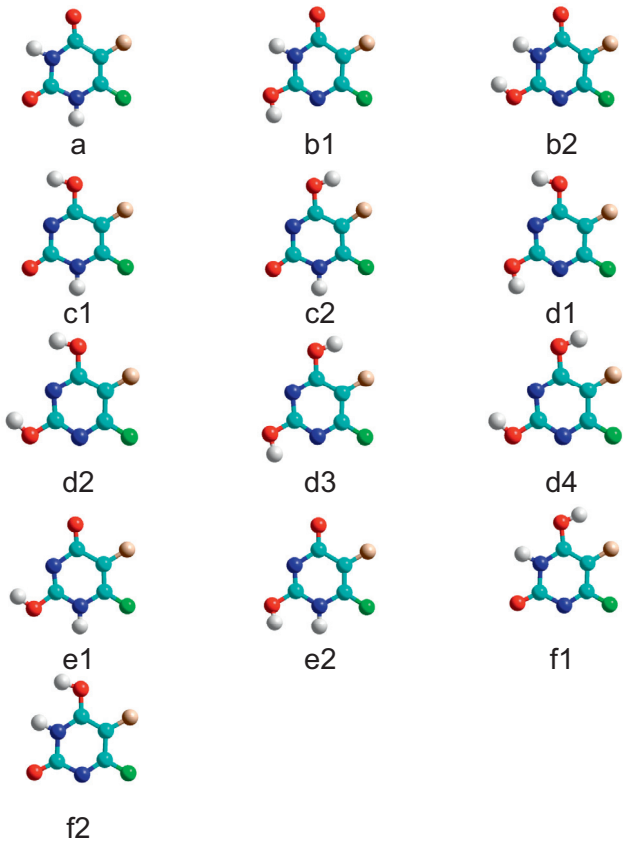


**Fig. 3.** Representative structures based on theoretical calculations at the B3LYP/6-31G(d) level of theory of the 13 most stable tautomeric conformations of neutral uracil (U) and the halouracils (*x*U), where *x*U = 5FU, 5ClU, 5BrU, 5IU, and 6ClU. The nucleobases are oriented as in Fig. 1. The 5-substituents (gold) represent H, F, Cl, Br, and I, whereas the 6-substituents (green) represent H and Cl. (For interpretation of the references to color in this figure legend, the reader is referred to the web version of this article.)

24.6 kJ/mol for $Na^+$(5FU), 25.7 kJ/mol for $Na^+$(5ClU) and $Na^+$(5BrU), and 25.8 kJ/mol for $Na^+$(5IU) above the ground-state $\mathbf{A^2}$ conformer. The first-excited conformers of the $Na^+$(5*x*U) complexes are the **C** conformers, which lie 16.6 kJ/mol above the ground-state $\mathbf{A^2}$ conformers for $Na^+$(5FU), 18.0 kJ/mol for $Na^+$(5ClU), 17.3 kJ/mol for $Na^+$(5BrU), and 19.1 kJ/mol for $Na^+$(5IU). These conformers result from the sodium cation chelating with the O2 and N3 atoms of the **c2** conformer. In these structures protons are bound to the N1, O4, and C6 atoms with the O4H atom oriented toward the 5-halo-substituent. These conformers could also be generated by binding of the sodium cation at the O2 position of the **a** conformers and proton transfer from the N3 to O4 position. The **C** conformers exemplify the stabilization of minor tautomers upon sodium cationization as the relative Gibbs free energies at 298 K decrease from 63.7 kJ/mol for neutral **c2** to 16.5 kJ/mol for sodium cationized **C** in $Na^+$(5FU) as compared to the **a** and $\mathbf{A^2}$ ground-state conformers of these species, respectively. Stabilization of the minor **c2** tautomer is also found for the other $Na^+$(5*x*U) complexes with the relative Gibbs free energy at 298 K decreasing from 61.8 kJ/mol for 5ClU to 18.0 kJ/mol for $Na^+$(5ClU), from 61.9 kJ/mol for 5BrU to 17.3 kJ/mol for $Na^+$(5BrU), and from 64.9 kJ/mol for 5IU to 19.1 kJ/mol for $Na^+$(5IU). In addition to these two low-energy conformers, 32 higher lying stable conformers were calculated for $Na^+$(5FU), 34 for $Na^+$(5ClU), 32 for $Na^+$(5BrU), and 29 for $Na^+$(5IU). The relative Gibbs free energies of these higher-energy conformers vary from 21.8 to

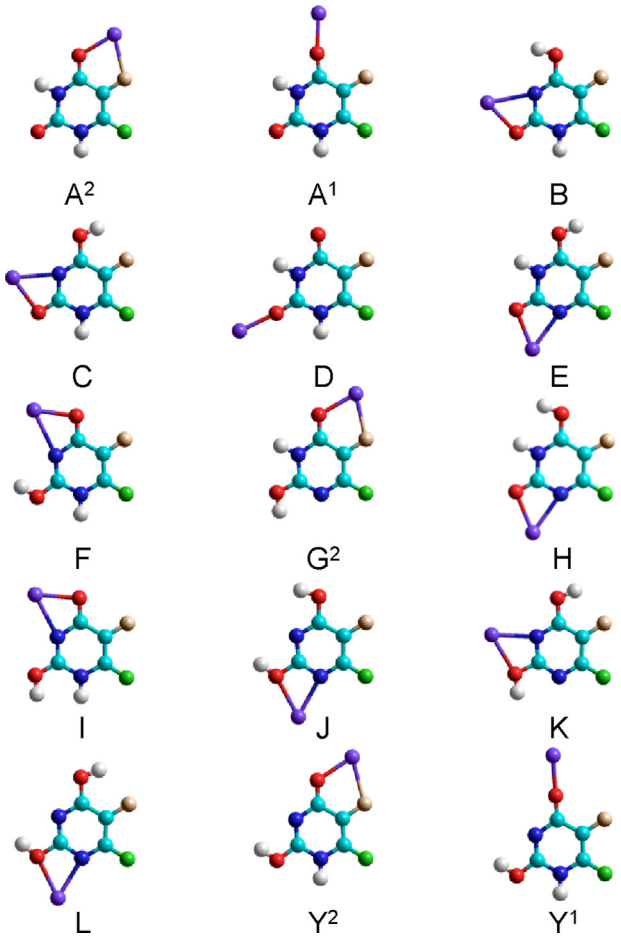


**Fig. 4.** Representative structures based on theoretical calculations at the B3LYP/6-31G(d) level of theory of the 13 most stable tautomeric conformations of sodium cationized uracil, $Na^+$(U), and the halouracils, $Na^+$ (*x*U), where *x*U = 5FU, 5ClU, 5BrU, 5IU, and 6ClU. The nucleobases are oriented as in Fig. 1. The 5-substituents (gold) represent H, F, Cl, Br, and I, whereas the 6-substituents (green) represent H and Cl. (For interpretation of the references to color in this figure legend, the reader is referred to the web version of this article.)

214.6 kJ/mol as compared to the ground-state **A²** conformer for $Na^+$(5FU), 25.7–208.1 kJ/mol for $Na^+$(5ClU), 25.7–200.1 kJ/mol for $Na^+$(5BrU), and 25.8–205.6 kJ/mol for $Na^+$(5IU) (see Fig. S2 of the Supplementary Information).

### 3.2.2. $Na^+$(6ClU)

Similar to that found for the $Na^+$(5*x*U) complexes, the ground-state structure of $Na^+$(6ClU) is the **A¹** conformer shown in Fig. 4 and Fig. S2 resulting from sodium binding at the O4 position to the **a** conformer of 6ClU. In this structure protons are bound to the N1, N3, and C5 atoms. The first-excited conformer of $Na^+$(6ClU) is the **B** conformer, which lies 14.7 kJ/mol above the ground-state conformation. This conformer results from the sodium cation chelating with the O2 and N3 atoms of the **c1** conformer with the protons bound to the N1 and O4 atoms oriented toward the N3 atom. The **E** conformer lies 16.1 kJ/mol above the ground-state **A¹** conformer. This conformer involves chelation of the sodium cation with O2 and N1 of the **f1** conformer with the protons bound to the N3 and O4 atoms oriented away from the N3 atom. Rotation of the 4-hydroxyl group of the **B** conformer away from the sodium cation results in **C** conformer, which lies 16.6 kJ/mol above the ground-state **A¹** conformer. This conformer results from the sodium cation chelating with the O2 and N3 atoms of the **c2** conformer with the protons bound to the N1 and O4 atoms oriented away from the N3 atom. The

**Table 1**
Stable low-energy tautomers of the $Na^+$(U) and $Na^+$(*x*U) complexes and their relative enthalpies and Gibbs free energies at 298 K.[a]

| Complex | Tautomer | $\Delta H_{298}$ (kJ/mol) | $\Delta G_{298}$ (kJ/mol) |
|---|---|---|---|
| $Na^+$(U) | $A^2$ | 0.0 | 0.0 |
| | B | 10.1 | 13.6 |
| | C | 11.0 | 15.2 |
| | D | 16.6 | 16.2 |
| | E | 26.3 | 30.4 |
| | F | 30.0 | 32.8 |
| | $G^1$ | 35.9 | 36.5 |
| | H | 40.4 | 43.9 |
| | I | 45.9 | 48.4 |
| | J | 45.8 | 49.7 |
| | K | 56.6 | 60.2 |
| | L | 59.8 | 63.6 |
| $Na^+$(5FU) | $A^2$ | 0.0 | 0.0 |
| | C | 15.6 | 16.5 |
| | $G^2$ | 23.7 | 21.8 |
| | D | 24.3 | 24.6 |
| | B | 25.5 | 25.4 |
| | $Y^2$ | 32.5 | 32.5 |
| | F | 34.8 | 34.4 |
| | E | 35.0 | 35.8 |
| | I | 50.1 | 50.0 |
| | J | 51.8 | 52.6 |
| | K | 53.0 | 53.7 |
| | L | 55.3 | 56.2 |
| $Na^+$(5ClU) | $A^2$ | 0 | 0 |
| | C | 16.3 | 18.0 |
| | D | 27.5 | 25.7 |
| | $G^2$ | 25.7 | 26.6 |
| | B | 27.4 | 28.2 |
| | $Y^1$ | 35.7 | 31.7 |
| | E | 32.3 | 33.7 |
| | $Y^2$ | 35.5 | 34.8 |
| | F | 39.3 | 39.6 |
| | I | 54.2 | 54.9 |
| | K | 55.4 | 56.8 |
| | J | 55.9 | 57.5 |
| $Na^+$(5BrU) | $A^2$ | 0 | 0 |
| | C | 16.3 | 17.3 |
| | D | 28.4 | 25.7 |
| | $G^2$ | 25.7 | 26.3 |
| | B | 27.9 | 28.0 |
| | E | 31.6 | 32.5 |
| | $Y^2$ | 36.4 | 36.5 |
| | F | 40.6 | 40.0 |
| | I | 55.3 | 55.2 |
| | K | 55.8 | 56.4 |
| | J | 57.0 | 57.7 |
| | H | 57.4 | 57.9 |
| $Na^+$(5IU) | $A^2$ | 0 | 0 |
| | C | 17.2 | 19.1 |
| | D | 27.6 | 25.8 |
| | $G^2$ | 27.0 | 27.9 |
| | B | 26.9 | 28.0 |
| | E | 31.2 | 33.2 |
| | $Y^2$ | 37.0 | 36.7 |
| | F | 40.2 | 40.7 |
| | I | 54.8 | 55.7 |
| | H | 56.0 | 57.5 |
| | J | 57.2 | 59.0 |
| | K | 57.4 | 59.1 |
| $Na^+$(6ClU) | $A^2$ | 0 | 0 |
| | B | 11.7 | 14.7 |
| | E | 12.4 | 16.1 |
| | C | 12.7 | 16.6 |
| | D | 17.8 | 17.9 |
| | $G^2$ | 25.0 | 25.7 |
| | H | 26.4 | 29.9 |
| | F | 32.9 | 35.8 |
| | J | 34.6 | 38.0 |
| | K | 47.0 | 50.4 |
| | I | 47.9 | 50.9 |
| | L | 48.4 | 51.8 |

[a] Calculations were performed at the B3LYP/6-311+G(2d,2p)//B3LYP/631G(d) level of theory. Conformation designations are based on the structures shown in Fig. 4 and Fig. S2.

**D** conformer, which lies 17.9 kJ/mol above the ground-state $\mathbf{A^1}$ conformer, results from binding of the sodium cation at the O2 position of the **a** conformer. Sodium cationization of 6ClU stabilizes multiple minor tautomers to relative Gibbs free energies at 298 K below 20 kJ/mol. The relative Gibbs free energy at 298 K decreases from 44.9 kJ/mol for neutral **c1** to 14.7 kJ/mol for sodium cationized **B**, from 64.2 kJ/mol for neutral **f1** to 16.1 kJ/mol for sodium cationized **E**, and from 70.2 kJ/mol for neutral **c2** to 16.6 kJ/mol for sodium cationized **C**. In addition to these low-energy conformers, 22 higher-energy conformers were calculated with relative Gibbs free energies varying from 25.7 to 208.6 kJ/mol as compared to the ground-state $\mathbf{A^1}$ conformer (see Fig. S2 of the Supplementary Information).

## 4. Discussion

### *4.1. Comparison of experimental IRMPD and theoretical IR spectra of $Na^+$(5ClU)*

The experimentally measured IRMPD action spectrum and theoretical linear IR spectra, calculated at the B3LYP/6-31G* level of theory, for the three most stable tautomeric conformations of $Na^+$(5ClU) are compared in Fig. 5. Also included in Fig. 5 are the structures and B3LYP/6-311+G(2d,2p) relative Gibbs free energies of these species at 298 K. This comparison shows good agreement between the measured IRMPD action spectrum and the calculated linear IR spectra for the ground-state $\mathbf{A^2}$ conformer. The intense band at 1808 $cm^{-1}$ is blue shifted by 3 $cm^{-1}$ to 1811 $cm^{-1}$ in the theoretical IR spectrum, whereas all other features are red shifted by up to 35 $cm^{-1}$ suggesting that theory may be underestimating the frequency of these spectral features. The theoretical linear IR spectrum of the first excited **C** conformer exhibits several features that allow for differentiation from the ground-state $\mathbf{A^2}$ conformer. A new band is observed at ~1528 $cm^{-1}$ and the intense feature observed near ~1800 $cm^{-1}$ is absent for the **C** conformer. In addition, the intense peak at ~1668 $cm^{-1}$ for the $\mathbf{A^2}$ conformer is blue shifted by 23 $cm^{-1}$. The blue shifting of this intense peak would cause further broadening of the corresponding feature in the measured IRMPD action spectrum if this conformer was accessed experimentally. In addition, the 1413 $cm^{-1}$ band (blue shifted by ~33 $cm^{-1}$ from 1380 $cm^{-1}$ for the ground-state $\mathbf{A^2}$ conformer) and the 1450 $cm^{-1}$ band (red shifted by ~23 $cm^{-1}$ from 1473 $cm^{-1}$ for the ground-state) would appear as severe broadening or new features in the measured IRMPD action spectrum. These differences indicate that the **C** conformer does not contribute to the measured IRMPD action spectrum. The estimated Maxwell-Boltzmann population of conformer **C** at 298 K is only ~0.1%, providing further support for the conclusion that this conformer does not contribute measurably to the IRMPD action spectrum. The second excited **D** conformer of $Na^+$(5ClU) lies 25.7 kJ/mol higher in free energy than the ground-state $\mathbf{A^2}$ conformer, and involves binding of the sodium cation to the O2 carbonyl oxygen atom of the canonical **a** tautomer. As compared to the ground-state $\mathbf{A^2}$ conformer, the intense band at 1808 $cm^{-1}$ is red shifted by 67 $cm^{-1}$, whereas the bands at ~1668 and 1602 $cm^{-1}$ are blue shifted by 31 and 18 $cm^{-1}$, respectively, for binding of sodium at O2 versus O4. These band shifts indicate that experimentally accessed structures bound at the O4 and O2 positions should be readily distinguished by their IRMPD spectra. Theoretical energetics verify that the ground-state $\mathbf{A^2}$ conformer of $Na^+$(5ClU) is the canonical **a** tautomer with $Na^+$ bound to the O4 carbonyl oxygen atom. As with the **C** conformer, these band shifts would appear as shoulders, severely broadened, or even new features, in the measured IRMPD action spectrum. The absence of new or broadened features indicates that the **D** conformer does not contribute measurably to IRMPD action spectrum.

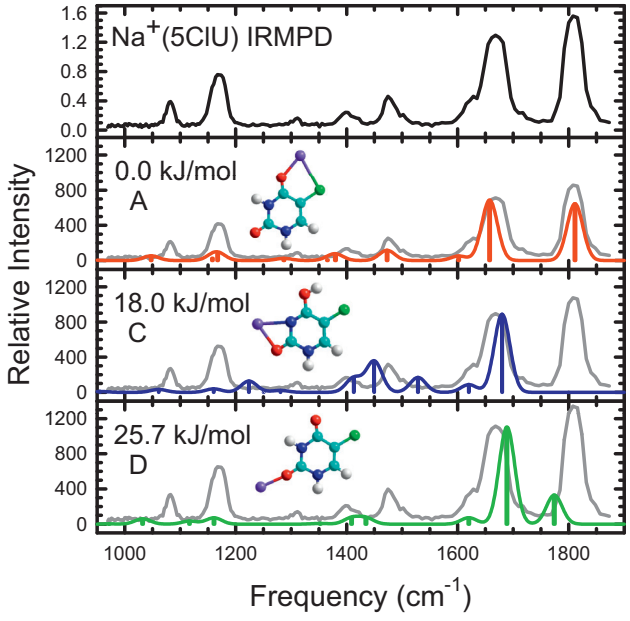


**Fig. 5.** Comparison of the measured IRMPD action spectrum of $Na^+$(5ClU) and the linear IR spectra predicted for the three most stable conformers of $Na^+$(5ClU) calculated at the B3LYP/6-31G(d) level of theory. The structures and B3LYP/6-311+G(2d,2p) relative Gibbs free energies at 298 K of each conformer are also shown. To facilitate comparison of the measured and computed spectra, the IRMPD spectrum is overlaid (in grey) with each of the computed spectra and scaled to match the intensity of the C=O4 carbonyl stretch. (For interpretation of the references to color in this figure legend, the reader is referred to the web version of this article.)

### *4.2. Comparison of $Na^+$(5ClU) to $Na^+$(5FU), $Na^+$(5BrU), and $Na^+$(5IU)*

The experimentally measured IRMPD action spectra and theoretical linear IR spectra, calculated at the B3LYP/6-31G* level of theory, for the two most stable tautomeric conformations $\mathbf{A^2}$ and **C**, and the canonical O2 sodium cation binding **D** conformer of the $Na^+$(5FU), $Na^+$(5BrU), and $Na^+$(5IU) complexes are included in Figs. S3–S5 of the Supplementary Information. Also included in Figs. S3–S5 are the structures and B3LYP/6-311+G(2d,2p) relative Gibbs free energies of these species at 298 K. Highly parallel behavior is found across these $Na^+$(5*x*U) complexes and the experimental and theoretical results for $Na^+$(5ClU). However, the relative stabilities of the second and third excited conformers, **D** and $\mathbf{G^2}$, differ for $Na^+$(5FU) as compared to the other $Na^+$(5*x*U) complexes, where the $\mathbf{G^2}$ conformer is 5–6 kJ/mol more stable for $Na^+$(5FU). A new feature in the IR spectra of the **C** conformers appears between 1552 and 1518 $cm^{-1}$ and decreases in frequency as the size of the halogen substituent increases. The bound carbonyl stretch of the **C** conformers is blue shifted, by between 18 and 29 $cm^{-1}$, with the largest shifts observed for the largest halogen substituents. The band appearing between 1394 and 1374 $cm^{-1}$ in the ground-state $\mathbf{A^2}$ conformers, exhibits increased blue shifting in the **C** conformers from 19 to 36 $cm^{-1}$ as the size of the halogen substituent increases. The band appearing between 1482 and 1468 $cm^{-1}$ in the ground-state $\mathbf{A^2}$ conformers, exhibits increased red shifting for the **C** conformers as the size of the halogen substituent increases. In the IR spectra of the **D** conformers the free carbonyl stretch is red shifted by 34–44 $cm^{-1}$ as compared to the ground-state $\mathbf{A^2}$ conformer. In contrast, the free carbonyl stretch of conformer **D** is blue shifted by 24–39 $cm^{-1}$ as compared to the ground-state $\mathbf{A^2}$ conformer. In both cases, the magnitude of the frequency shifting increases with the size of the halogen substituent. The C=C stretch is red shifted by

18 $cm^{-1}$ for both $Na^+$(5ClU) and $Na^+$(5BrU), 20 $cm^{-1}$ for ($Na^+$(5IU), and 22 $cm^{-1}$ for $Na^+$(5FU).

As observed for $Na^+$(5ClU), there is a slight red shifting of all features except the free carbonyl stretch in the theoretical IR spectra for all of the $Na^+$(5*x*U) complexes. The red shifting, as observed in $Na^+$(5ClU), is less severe for the bound carbonyl stretch, N1H in plane rocking, and the C6–N1 stretch as compared to other spectral features in all cases except $Na^+$(5FU). The free carbonyl stretch, as in the case of $Na^+$(5ClU), is blue shifted by 3 $cm^{-1}$ to 1811 $cm^{-1}$ in the theoretical IR spectra for the other $Na^+$(5*x*U) complexes.

### 4.3. Comparison of experimental IRMPD and theoretical IR spectra of $Na^+$(6ClU)

The experimentally measured IRMPD action spectrum and theoretical linear IR spectra, calculated at the B3LYP/6-31G* level of theory, for the five most stable tautomeric conformations of $Na^+$(6ClU) are compared in Fig. 6. Also included in Fig. 6 are the structures and B3LYP/6-311+G(2d,2p) relative Gibbs free energies of these species at 298 K. This comparison shows very good agreement between the measured IRMPD action spectrum and the calculated linear IR spectrum for the ground-state **A¹** conformer. Red shifting of all features by 2–33 $cm^{-1}$ except the free carbonyl stretch at

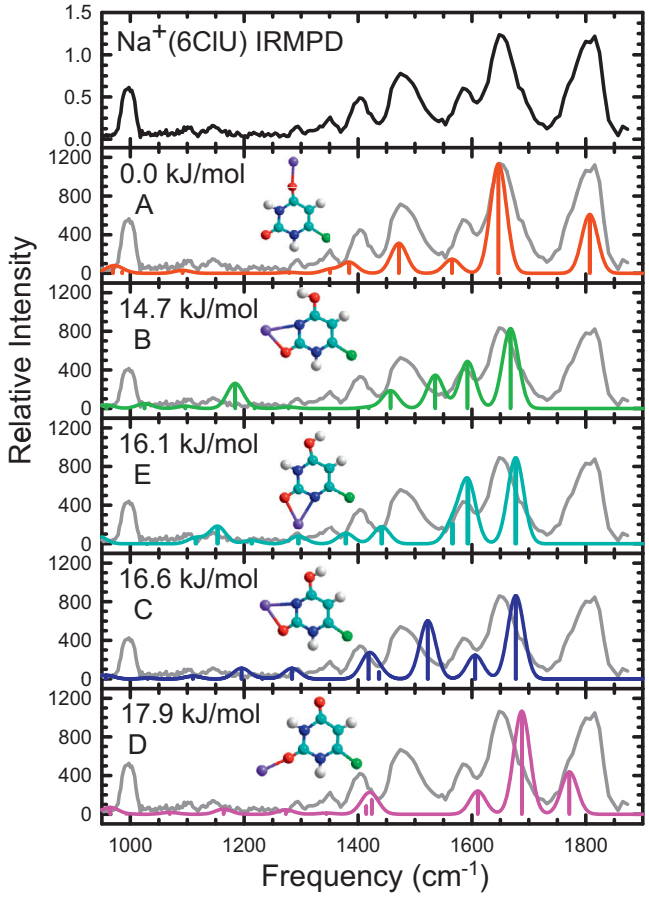


**Fig. 6.** Comparison of the measured IRMPD action spectrum of $Na^+$(6ClU) and the linear IR spectra predicted for the five most stable conformers of $Na^+$(6ClU) calculated at the B3LYP/6-31G(d) level of theory. The structures and B3LYP/6-311+G(2d,2p) relative Gibbs Free energy at 298 K of each conformer are also shown. To facilitate comparison of the measured and computed spectra, the IRMPD spectrum is overlaid (in grey) with each of the computed spectra and scaled to match the intensity of the C=O4 carbonyl stretch. (For interpretation of the references to color in this figure legend, the reader is referred to the web version of this article.)

~1808 $cm^{-1}$ and the N3–H in-plane rocking at ~1350 $cm^{-1}$ is again observed. This suggests theory is underestimating the frequency of the red shifted spectral features. There are also additional features present in the measured IRMPD spectrum compared to the theoretically calculated IR spectrum for the ground-state **A¹** conformer. $Na^+$(6ClU) exhibits five conformations below 20 kJ/mol, whereas the other $Na^+$(5*x*U) complexes exhibit only two. Thus, halogenation at the 6-position leads to increased stabilization of minor tautomers. All excited conformers exhibit blue shifting of the bound carbonyl stretch and red shifting of the C–X stretch. The first and third excited conformations, **B** and **C**, differ only by the rotation of the 4-hydroxyl group. Both conformations exhibit bands at ~1190 and ~1530 $cm^{-1}$ that are not observed in the measured IRMPD spectrum. The 298 K Maxwell–Boltzmann population calculated for the first excited state is ~0.26%. The second excited conformation exhibits new bands at ~1380 and ~1440 $cm^{-1}$, and blue shifting of the bound carbonyl from ~1650 to ~1675 $cm^{-1}$, which would appear as new features or broadening in the measured IRMPD action spectrum. The forth excited **D** conformer, which involves sodium cation binding to the O2 carbonyl oxygen atom of the canonical **a** tautomer, should be readily differentiated from the O4 binding ground-state **A¹** conformer. The position of the free carbonyl stretch red shifts for O2 binding by 36 $cm^{-1}$ versus O4 binding, whereas the sodium bound carbonyl and C=C stretches blue shift by 41 and 45 $cm^{-1}$, respectively. These band shifts indicate that experimentally accessed structures bound at the O4 or O2 positions should be readily distinguished by their IRMPD spectra. Theoretical energetics verify that the ground-state **A¹** conformer of these complexes is the canonical **a** tautomer with $Na^+$ bound at the O4 carbonyl oxygen atom. The relative stabilities suggest any excited conformers that may be accessed would make very minor contributions to the measured IRMPD spectrum. Severe broadening observed in the experimentally measured IRMPD spectrum suggests that excited conformers are indeed accessed and contribute to the measured IRMPD spectrum. This broadening in the measured IRMPD spectrum of $Na^+$(6ClU) is present at frequencies where the low-energy excited conformers exhibit high intensity bands, suggesting that the observed broadening of many spectral features is likely due to minor contributions of excited conformers accessed in the experiments, and thus theory may be underestimating the stabilities of these excited conformers for the $Na^+$(6ClU) complex.

Observed band positions (in $cm^{-1}$) of the vibrational modes of the $Na^+$(*x*U) complexes in the IR fingerprint region are compared in Table 2. Assignments are made based on comparison of the IRMPD action spectra and theoretical IR spectra of the ground-state canonical **A²** and **A¹** conformers optimized at the B3LYP/631G(d) level of theory. Comparison of the IRMPD action spectrum to the theoretical IR spectrum of the ground-state **A²** and **A¹** conformers of the $Na^+$(*x*U) complexes suggests that the absorption bands at ~1810 and ~1650 $cm^{-1}$ correspond to the C4=O and C2=O stretching, respectively. The small shoulder at ~1600 $cm^{-1}$ corresponds to C5=C6 stretching. The small feature at ~1475 $cm^{-1}$ corresponds to N1–H rocking. The small feature at 1375 $cm^{-1}$ is composed of two weak absorption bands that correspond to N3–C4–C5 asymmetric stretching and N3–H rocking. The small feature at ~1300 $cm^{-1}$ corresponds to C6–H rocking of $Na^+$(5*x*U) complexes and N1–H and C5–H symmetric rocking of $Na^+$(6ClU). The feature at 1150 $cm^{-1}$ is composed of two weak absorption bands that correspond to N1–H and C6–H asymmetric rocking and C2–N3–C4 asymmetric stretching in $Na^+$(5FU) and $Na^+$(5IU). The feature at 1150 $cm^{-1}$ is composed of two weak absorption bands that correspond to N1–C6 stretching and C2–N3–C4 asymmetric stretching of $Na^+$(5ClU) and $Na^+$(5BrU). The feature at 1092 $cm^{-1}$ in $Na^+$(6ClU) corresponds to N1–C6 stretching and C5–H rocking. The feature at 1279 $cm^{-1}$ in $Na^+$(6ClU) corresponds to N1–H and C5–H symmetric rocking. The feature at

**Table 2**
Observed band positions (in $cm^{-1}$) of the vibrational modes of the $Na^+(xU)$ complexes in the IR fingerprint region.[a]

| Vibrational mode | $Na^+$(5FU) | $Na^+$(5ClU) | $Na^+$(5BrU) | $Na^+$(5IU) | $Na^+$(6ClU) |
|---|---|---|---|---|---|
| C–X stretch | 1203 | 1048 | 1022 | 1004 | 970 |
| N3–C4–C5 symmetric stretch | – | – | – | – | 986 |
| C2–N3–C4 asymmetric stretch | 1161 | 1158 | 1158 | 1160 | – |
| N1–H and C6–H asymmetric rocking | 1127 | – | – | 1162 | – |
| N1–C6 stretch | – | 1167 | 1165 | – | – |
| N1–C6 stretch and C5–H rocking | – | – | – | – | 1092 |
| N1–H and C5–H symmetric rocking | – | – | – | – | 1279 |
| C6–H rocking | 1295 | 1287 | 1290 | 1291 | – |
| N3–H rocking | 1361 | 1365 | 1366 | 1366 | 1351 |
| N3–C4–C5 asymmetric stretch | 1394 | 1380 | 1377 | 1374 | 1385 |
| N1–H rock | 1482 | 1473 | 1470 | 1468 | 1472 |
| C5=C6 stretch | 1643 | 1602 | 1597 | 1585 | 1565 |
| C4=O stretch | 1664 | 1658 | 1657 | 1650 | 1647 |
| C2=O stretch | 1811 | 1811 | 1811 | 1811 | 1807 |

[a] Assignments based on comparison of the IRMPD action spectra and theoretical IR spectra of the ground-state canonical diketo **A²** and **A¹** conformers optimized at the B3LYP/6-311+G(2d,2p)//B3LYP/631G(d) level of theory.

1203 $cm^{-1}$ in $Na^+$(5FU), 1048 $cm^{-1}$ in $Na^+$(5ClU), 1022 $cm^{-1}$ in $Na^+$(5BrU), and 1004 $cm^{-1}$ in $Na^+$(5IU), corresponds to C5–X stretching. The feature at 970 $cm^{-1}$ in $Na^+$(6ClU) corresponds to C6–X stretching and N3–C4–C5 symmetric stretching.

### 4.4. Effect of halogenation on the IRMPD spectra

The effect of halogenation on the IRMPD spectra of sodium cationized uracil and the halouracils can be seen in the comparison of Fig. 2. The frequency of the free carbonyl (C2=O) stretch is preserved for all of the $Na^+(xU)$ complexes as the halogen substituent clearly has no direct interaction with this carbonyl moiety. In contrast and not surprisingly, the bound carbonyl (C4=O) stretch exhibits systematic shifts that vary with the size of the halogen substituent. The C4=O stretch observed at ~1659 $cm^{-1}$ for $Na^+$(U) is blue shifted to 1675 $cm^{-1}$ for $Na^+$(5FU), and red shifts by between 7 and 20 $cm^{-1}$ relative to $Na^+$(5FU) for the other $Na^+(5xU)$ complexes, with the largest shifts observed for the largest halogen substituents. The C5=C6 stretch is not resolved from the C4=O stretch for $Na^+$(U) and $Na^+$(5FU). The C5=C6 stretch observed at 1675 $cm^{-1}$ for $Na^+$(5ClU) red shifts by between 20 and 26 $cm^{-1}$ for the other $Na^+(5xU)$ complexes, with the largest shifts observed for the largest halogen substituents. The N1–H rocking observed at ~1491 $cm^{-1}$ for $Na^+$(U), blue shifts to ~1496 $cm^{-1}$ for $Na^+$(5FU), but then red shifts by between 22 and 32 $cm^{-1}$ relative to $Na^+$(5FU) in the spectra of the other $Na^+(5xU)$ complexes, with the largest shifts again being observed for the largest halogen substituents. The two weak absorption bands that correspond to N3–C4–C5 asymmetric stretching and N3–H rocking observed at 1417 $cm^{-1}$ for $Na^+$(U) and $Na^+$(5FU) red shift by between 14 and 19 $cm^{-1}$ for the other $Na^+(5xU)$ complexes, with the largest shifts again observed for the largest halogen substituents. The C6–H rocking observed at ~1328 $cm^{-1}$ for $Na^+$(U) red shifts to ~1295 $cm^{-1}$ for $Na^+$(5FU) and further red shifts by 4–8 $cm^{-1}$ for the other $Na^+$(5XU) complexes. Ring stretching observed at 1174 $cm^{-1}$ for $Na^+$(5ClU) red shifts by 7 $cm^{-1}$ for $Na^+$(5BrU), 10 $cm^{-1}$ for $Na^+$(5IU), and 23 $cm^{-1}$ for $Na^+$(5FU). The C5–X stretch exhibits the largest shift due to the varying size of the halogen substituent. The C5–X stretch is observed at 1231 $cm^{-1}$ for $Na^+$(5FU), 1083 $cm^{-1}$ for $Na^+$(5ClU), 1074 $cm^{-1}$ for $Na^+$(5BrU), and 1035 $cm^{-1}$ for $Na^+$(5IU). Broadening of the features observed in the IRMPD action spectra decreases with increasing size of the halogen substituent. Thus, the overall impact of halogenation on the IRMPD spectra is generally most pronounced for $Na^+$(5FU), and decreases relatively systematically with increasing size of the halogen substitutent.

### 4.5. Effect of sodium cationization on the IR spectra

The IRMPD action spectra of the $Na^+(xU)$ complexes measured in this work and the theoretical linear IR spectra, calculated at the B3LYP/6-31G(d) level of theory, for the ground-state tautomeric conformations of the neutral 5-halouracils and 6-chlorouracil are compared in Fig. S6. Also included in Fig. S6 are the neutral ground-state canonical tautomeric conformations. Sodium cationization of the neutral halouracils causes shifting of several of the spectral features. Sodium cationization results in a blue shift of the O2 carbonyl stretch by 30–34 $cm^{-1}$ with the largest shifts observed for the smallest halogen substituents. Not surprisingly, sodium cationization results in a large red shift of the O4 carbonyl stretch (the binding site) by 67–81 $cm^{-1}$ with the largest shifts observed for the largest halogen substituents, and is red shifted the furthest by 88 $cm^{-1}$ for $Na^+$(6ClU). Sodium cationization results in a red shift of the C=C stretch by up to 8 $cm^{-1}$ with the largest shifts observed for the smallest halogen substituents, whereas a much larger shift of 20 $cm^{-1}$ occurs for $Na^+$(6ClU). In the case of $Na^+$(5FU), the C=C stretch is not resolved from the O4 carbonyl stretch. Sodium cationization results in a blue shift of the peak at ~1475 $cm^{-1}$ by 25–45 $cm^{-1}$, with the largest shifts observed for the smallest halogen substituents. Sodium cationization results in a blue shift of the peak at ~1400 $cm^{-1}$ by 39 $cm^{-1}$ for $Na^+$(5FU), 47 $cm^{-1}$ for $Na^+$(5ClU), 49 $cm^{-1}$ for $Na^+$(5BrU), 46 $cm^{-1}$ for $Na^+$(5IU), and by 53 $cm^{-1}$ for $Na^+$(6ClU). Sodium cationization results in a red shift of the peak at ~1310 $cm^{-1}$ by 2–39 $cm^{-1}$, with the largest shifts observed for the smallest halogen substituents. Sodium cationization results in a blue shift of the peak at ~1150 $cm^{-1}$ by 7 $cm^{-1}$ for $Na^+$(5FU), 14 $cm^{-1}$ for $Na^+$(5ClU) and $Na^+$(5BrU), and 8 $cm^{-1}$ for $Na^+$(5IU). Sodium cationization results in a red shift of the C–X stretch by 4 $cm^{-1}$ for $Na^+$(5FU), and a blue shift of 45 $cm^{-1}$ for $Na^+$(5ClU), 44 $cm^{-1}$ for $Na^+$(5BrU), 46 $cm^{-1}$ for $Na^+$(5IU), and 143 $cm^{-1}$ for $Na^+$(6ClU). Clearly, sodium cationization has a significant impact on the band positions of all features leading to facile differentiation from the neutral halouracils (see Fig. S2 of the Supplementary Information).

### 4.6. Comparison to $H^+(xU)$, $H^+(xSU)$, and $Na^+(xSU)$ systems previously investigated

Previous studies of the protonated and sodium cationized forms of uracil and a variety of substituted uracils including thioketouracils and methylthioketouracils demonstrate stabilization of minor tautomers of these nucleobases as a result of protonation and sodium cationization [25,28–32]. In addition,

protonation of halouracils has similarly shown stabilization of minor tautomers [26]. The effects of protonation are more significant in the preferential stabilization of minor tautomers than that of sodium cationization. Sodium cationization typically favors canonical ground-state tautomers with few exceptions. The present theoretical results provide additional evidence for the preferential stabilization of minor tautomers due to sodium cationization of the halouracils. In comparison with protonation of halouracils the effects due to sodium cationization are again less dramatic. Protonation of the halouracils leads to a greater increase in the stability of minor tautomers than sodium cationization such that minor tautomers become the ground-state conformations, whereas the canonical tautomers remain the ground-state conformers of the sodium cationized halouracils.

### 4.7. Comparison with CID work

The results of this work are consistent with previous energy-resolved CID studies of alkali metal cationized uracil and methyl-, thioketo-, and halo-substituted uracils from guided ion beam tandem mass spectrometry studies [25,29–31]. The ground-state structures of uracil and the modified uracils almost exclusively involve $Na^+$ binding to the O4 carbonyl oxygen atom of the canonical **a** tautomer. The $Na^+$(4SU) complex is the only system examined thus far where this is not the case, and binding at O2 is preferred. Theoretical calculations using the MP2(full)/6-31G* optimized geometrics of $Na^+$(*x*U) complexes performed in the previous CID study for the uracil and halouracil complexes similarly find the canonical **a** tautomer as the ground-state for these systems with binding at the O4 position. [31] The dissociation behavior observed upon IR irradiation in the current study, corresponding to loss of the intact neutral nucleobase, is also consistent with the dominant CID process for alkali metal cationized uracil and methyl-, thioketo-, and halo-substituted uracils previously observed [25,29–31].

## 5. Conclusions

IRMPD action spectra of the sodium cationized halouracil complexes, $Na^+$(5FU), $Na^+$(5ClU), $Na^+$(5BrU), $Na^+$(5IU), and $Na^+$(6ClU), in the infrared fingerprint region extending from ~950 to 1900 $cm^{-1}$ have been obtained. The primary IRMPD pathways observed are consistent with those observed for uracil and thioketo-uracils in which dissociation leads to detection of the sodium cation and loss of the intact neutral nucleobase [32]. These results are also consistent with energy-resolved CID data for uracil and methyl-, thioketo-, and halo-substituted uracils from guided ion beam tandem mass spectrometry studies in our laboratory [25,29–31]. Comparison with linear IR spectra calculated at the B3LYP/6-31G(d) level of theory allow the experimentally accessed conformations to be identified. Based on the computed linear IR spectra, O2 versus O4 binding of the sodium cation should be easily differentiated. The band positions differ by at least 35 $cm^{-1}$ for the free carbonyl stretch, 25 $cm^{-1}$ for the sodium bound carbonyl stretch, and at least 19 $cm^{-1}$ for all C=C stretches. In all cases, the experimental IRMPD action spectra indicate preferential binding of the sodium cation to the O4 carbonyl oxygen atom of the canonical diketo **a** tautomer. The present results suggest that only a single conformer is accessed for all of the $Na^+$(5*x*U) complexes, whereas multiple conformers are accessed for the $Na^+$(6ClU) complex. Theoretical energetics verify that the ground-state structures of these complexes involve $Na^+$ binding to the O4 carbonyl oxygen atom of the canonical tautomer, with chelation to the halogen substituent providing additional stabilization for all of the 5-halouracils.

## Acknowledgments

Financial support for this work was provided by the National Science Foundation, Grants OISE-0730072 and CHE-1409420. C.M. K. also thanks the Wayne State University Honors Program for partial financial support via her Undergraduate Research and Creative Projects Award. We would also like to thank WSU C&IT for computer time and support. This work is part of the research program of FOM, which is financially supported by the Nederlandse Organisatie voor Wetenschapplelijk Onderzoek (NOW). The skillful assistance of the FELIX staff is gratefully acknowledged.

## Appendix A. Supplementary data

Supplementary data associated with this article can be found, in the online version, at http://dx.doi.org/10.1016/j.ijms.2014.07.016.

## References

[1] S. Denifl, S. Ptasińska, B. Gstir, P. Scheier, T.D. Märk, Int. J. Mass Spectrom. 232 (2004) 99.
[2] Q. Jiang, B.C. Blount, B.N. Ames, J. Biol. Chem. 278 (2003) 32834.
[3] W.P. Rowe, D.R. Lowy, N. Teich, J.W. Hartly, Proc. Natl. Acad. Sci. (U. S. A.) 69 (1972) 1033.
[4] P. Noordhuis, U. Holwerda, C.L. Van der Wilt, C.J. Van Groeningen, K. Smid, S. Meijer, H.M. Pinedo, G.J. Peters, Ann. Oncol. 15 (2004) 1025.
[5] J.B. Parker, J.T. Stivers, Biochemistry-US 50 (2011) 612.
[6] H. Sternglanz, C.E. Bugg, Biochim. Biophys. Acta 378 (1975) 1.
[7] S.M. Morris, Mutat. Res. 297 (1993) 39.
[8] C.H. Takimoto, D.B. Voeller, J.M. Strong, L. Anderson, E. Chu, C.J. Allegra, J. Biol. Chem. 268 (1993) 21438.
[9] J.P. Henderson, J. Byun, J. Takeshita, J.W. Heinecke, J. Biol. Chem. 278 (2003) 23522.
[10] C. Heidelberger, Prog. Nucleic Acid Res. Mol. Biol. 4 (1965) 1.
[11] U.P. Singh, B.N. Singh, A.K. Ghose, R.K. Singh, A. Sodhi, J. Inorg. Biochem. 44 (1991) 277.
[12] Y.H. Jang, L.C. Sowers, T. Cagin, W.A. Goddard III, J. Phys. Chem. A 105 (2001) 274.
[13] T. Nakijama, World J. Surg. 19 (1995) 570.
[14] Y. Shintani, M. Ohta, H. Hirabayashi, H. Tanaka, K. Iuchi, K. Nakagawa, H. Maeda, T. Kido, S. Miyoshi, H. Matsuda, Lung Cancer 45 (2004) 189.
[15] M. Sawicka, M. Kalinowska, W. Lewandowski, J. Pharm. Pharmacol. 56 (2004) 1067.
[16] J. Verheggen, A. Van Aerschot, L. Van Meervelt, J. Rozenski, L. Wiebe, R. Snoeck, G. Andrei, J. Balzarini, P. Claes, E. De Clercq, J. Med. Chem. 38 (1995) 826.
[17] A. Ghosh, R. Nayak, M.S. Shaila, Antiviral Res. 31 (1996) 35.
[18] A. Panagiotopoulou, N. Katsaros, N.G. Di Masi, G. Natile, Inorg. Chim. Acta 325 (2001) 73.
[19] M.T. Morgan, M.T. Bennett, A.C. Drohat, J. Biol. Chem. 282 (2007) 27578.
[20] R.H. Garrett, C.M. Grisham, Biochemistry, 3rd ed., Thomson Learning, Belmont, CA, 2005 Chapter 7 and 32.
[21] G.L. Eichhorn, L.C. Marzilli, Advances in Inorganic Biochemistry; Metal Ions in Genetic Information Transfer, Vol. 3, Elsevier Science, New York, 1981, pp. 1.
[22] A.M. Pyle, J. Biol. Inorg. Chem. 7 (2002) 679.
[23] Y.A. Shin, G.L. Eichhorn, Biopolymers 16 (1977) 225.
[24] W. Saenger, in: C.R. Canton (Ed.), Principles of Nucleic Acid Structure, Springer-Verlag, Boston, 1984.
[25] Z. Yang, M.T. Rodgers, Int. J. Mass Spectrom. 241 (2005) 225.
[26] K.T. Crampton, A.I. Rathur, Y.-w. Nei, G. Berden, J. Oomens, M.T. Rodgers, J. Am. Soc. Mass Spectrom. 23 (2012) 1469.
[27] J.-Y. Salpin, S. Guillaumont, J. Tortajada, L. MacAleese, J. Lemair, P. Maitre, ChemPhysChem 8 (2007) 2235.
[28] Y.-w. Nei, T.E. Akinyemi, J.D. Steill, J. Oomens, M.T. Rodgers, Int. J. Mass Spectrom. 297 (2010) 139.
[29] M.T. Rodgers, P.B. Armentrout, J. Am. Chem. Soc. 122 (2000) 8548.
[30] Z. Yang, M.T. Rodgers, J. Phys. Chem. A 110 (2006) 1455.
[31] Z. Yang, M.T. Rodgers, J. Am. Chem. Soc. 126 (2004) 16217.
[32] Y.-w Nei, T.E. Akinyemi, C.M. Kaczan, J.D. Steill, J. Oomens, M.T. Rodgers, Int. J. Mass Spectrom. 308 (2011) 191.
[33] J.J. Valle, J.R. Eyler, J. Oomens, D.T. Moore, A.F.G. van der Meer, G. von Heldon, G. Meijer, C.L. Hendrickson, A.G. Marshall, G.T. Blankley, Rev. Sci. Instrum. 76 (2005) 023103.
[34] N.C. Polfer, J. Oomens, D.T. Moore, G. von Heldon, G. Meijer, R.C. Dunbar, J. Am. Chem. Soc. 128 (2006) 517.
[35] N.C. Polfer, J. Oomens, Phys. Chem. Chem. Phys. 9 (2007) 3804.
[36] M.J. Frisch, G.W. Trucks, H.B. Schlegel, G.E. Scuseria, M.A. Robb, J.R. Cheeseman, J.A. Montgomery Jr., T. Vreven, K.N. Kudin, J.C. Burant, J.M. Millam, S.S. Iyengar, J. Tomasi, V. Barone, B. Mennucci, M. Cossi, G. Schalmani, N. Rega, G.A. Petersson, H. Nakatsuji, M. Hada, M. Ehara, K. Toyota, R. Fuuda, J. Hasegwa, M.

Ishida, T. Nakajima, Y. Honda, O. Kitao, H. Jaramillo, R. Gomperts, R.E. Stratmann, O. Yazyev, A.J. Austin, R. Cammi, C. Pomelli, J.W. Ochterski, P.Y. Ayala, K. Morokuma, G.A. Voth, P. Salvador, J.J. Dannenberg, V.G. Zakrzewski, S. Dapprich, A.D. Daniels, M.C. Strain, O. Farkas, D.K. Malick, A. Rabuck, K. Raghavachari, J.B. Foresman, J.V. Ortiz, Q.A.G. Cui Baboul, S. Clifford, J. Cioslowski, B.B. Stefanov, G.A. Lui Liashenko, P. Piskorz, I. Komaromi, R.L. Martin, D.J. Fox, T. Keith, M.A. Al-Laham, C.Y. Peng, A. Nanayakkara, M. Challacombe, P.M.W. Gill, B. Johnson, W. Chen, M.W. Wong, C. Gonzalez, J.A. Pople, Gaussian 03, Revision D.01, Gaussian, Inc., Pittsburgh, PA, 2005.
[37] P.J. Hay, W.R. Wadt, J. Chem. Phys. 82 (1985) 299.
[38] C.E. Check, T.O. Faust, J.M. Bailey, J.B. Wright, T.M. Gilbert, L.S. Sunderlin, J. Phys. Chem. A 105 (2001) 8111.
[39] J.B. Foresman, A.E. Frisch, Exploring Chemistry with Electronic Structure Methods, 2nd ed., Gaussian, Pittsburgh, PA, 1996, pp. 64.